

Visible light assisted photo catalytic degradation of eosin yellow using hetro atom functionalized TiO₂ nanomaterial

Desta Shumuye Meshesha^{a1}, Siva Rao Tirukkovallur^{a2*}, Matangi Ravi Chandra^{a3}, Sreedhar Bojja^b

^{a1}. Department of Chemistry, University of Gondar, Gondar, Ethiopia, 196

^{a1}, ^{a2*}, ^{a3}. Department of Inorganic and Analytical Chemistry, Andhra University, Visakhapatnam 530003, India.

^b. Department of Inorganic & Physical Chemistry Division, Indian Institute of Chemical Technology, Hyderabad 500007, India.

Corresponding author: Desta Shumuye

ABSTRACT

Eosin Yellow dye of 10ppm was successfully photodegraded using visible light active co-doped TiO₂ nanomaterial that was synthesized from 0.75wt% Ba & 0.25wt% Zr by the sol-gel method as photocatalyst under irradiation for 20 minutes and characterized by various advanced scientific instrumental techniques. X-ray diffraction showed that the prepared nanomaterial was in the anatase phase with 2theta (2Q) at 25.3°. UV-visible diffuse reflectance spectra analysis enlightened that the dopants found in the TiO₂ convey a significant absorption shift towards the visible region and their existence was confirmed by X-ray photoelectron spectral data. The formation of hydroxyl radical by the nanomaterial catalyst in aqueous solution under visible light irradiation was obtained quantitatively by the photoluminescence technique. Finally, the effects of different parameters in the photocatalytic degradation of eosin yellow were established in aqueous solution.

Keywords: - Eosin yellow, hydroxyl ion, photoluminescent.

Date of Submission: 01-09-2020

Date of Acceptance: 16-09-2020

I. INTRODUCTION

Industrial rebellion and the day to day human activities have influenced the flow, Storage of water, and the quality of available freshwater. Dyes are used in food, textiles, beverage industries, and printing processes and huge volumes of water consume by textile industries and generate huge quantities of colored dye effluents during the processes [1–3]. Natural streams and rivers can be extremely spoiled when untreated colored effluents are discharged to the water bodies that cause chemical as well as biochemical changes and consumes dissolved oxygen and destroy aquatic life [4–6]. Eosin Yellowish heterocyclic dye-containing bromine atoms, specifically used in the fields of dyeing, printing, leather, printing ink, and fluorescent pigment, etc, because of its vivid color. The traditional techniques, such as coagulation/flocculation, membrane separation (ultra-filtration, reverse osmosis), or absorption of activated carbon, are mostly based on the phase transfer mechanism of the pollutant.

Colored dyes owing to their complex chemical structures, they are resistant to

biodegradation and are hardly removed from effluents using conventional wastewater treatments. Among advanced oxidation processes (AOPs), semiconductor/ heterogeneous photocatalysis appears as the most emerging destructive technology with the possibility of using sunlight as the source of irradiation to initiate the destruction of organic pollutants [7]. Titanium dioxide (TiO₂) is the most widely used photocatalyst which is a newly growing technology and highly promising, cheap, stable, nontoxic, and efficient free from secondary pollutants for serving environmental purification and best appropriate photocatalyst is TiO₂ [8, 9]. Out of the incoming solar energy on the Earth's surface, only 4% can be utilized by titania because of the relatively high intrinsic bandgap of anatase TiO₂ (3.2 eV), The main drawback associated with its use is, the activated charge carriers before reaching the surface interaction with adsorbed molecules will undertake recombination leading to low photoactivity of TiO₂ within a nanosecond after their generation. Avoiding this limitation, and to get better light absorption features characteristics and to extend photocatalytic carrier lifetime, to extend the visible

light response of TiO₂ doping and co-doping of metals, nonmetals, or metal & nonmetal found to be most suitable [10- 13]. Nitrogen-doped TiO₂ was considered to be promising by reducing the bandgap making it visible light active photocatalyst and metal dopants facilitate the charge separation of e⁻/h⁺ and thus decrease their rate of recombination [14].

Studies on the Synthesis of a series of Zr,S co-doped TiO₂ (Zr-TiO₂-S) prepared by a modified sol-gel method were also developed for the degradation of pollutants[15]. Studied on the feasibility of a novel adsorbent composite photocatalyst, poly (pyrrole-co-aniline)-coated TiO₂/nanocellulose composite (P(Py-co-An)-TiO₂/NCC), to remove eosin yellow (EY) from aqueous solutions [16]. For having powders of homogenous concentrations synthesized at low temperatures with high purity under the stoichiometry control Sol-gel method is helpful [17]. Because of the significance of visible light-responsive photocatalyst, it is much honored to use a photocatalyst with appropriate particle size, phase, and other surface properties hence sol-gel method has been followed for the preparation of barium and zirconium co-doped TiO₂ (Ba & Zr co-doped TiO₂) nanomaterial.

1.1 Photocatalysts Synthesis.

A series of TiO₂ samples were prepared by co-doping with various amounts of Ba²⁺ and Zr⁴⁺ wt% in the range of 0.25 –1.25 wt% and undoped TiO₂ by sol-gel method. For undoped TiO₂ preparation, ethanol is taken as a solvent, and water was added to titanium tetrabutoxide (titanium precursor) for having hydrolysis and condensation reactions in presence of nitric acid. In the case of co-doped catalyst preparation, calculated quantities of barium nitrate and zirconyl nitrate, (precursors of Ba and Zr,) respectively were initially dissolved in ethanol along with water and the resultant solution was added drop by drop from the burette to the ethanol solution of Ti(OBu)₄ under vigorous stirring. After the addition is over, the colloidal suspension was allowed to stir for 60 min and aged for 48 hrs in the dark. The formed gel was dried in an oven at 100°C. Afterward, it was well-grounded and calcined at 450°C for 2 hrs in a muffle furnace and then cooled and grounded to form a homogenous powder.

1.2. Characterization of Photocatalysts. XRD spectra were recorded for 2θ from 20° to 80° with model Ultima IV, RIGAKU diffractometer using monochromatized CuKα radiation (λ = 1.541 Å) with a Germanium solid-state detector. The crystallite size of the nanoparticles was calculated from the Scherrer equation, XPS studies were done

using PHI quantum ESCA microprobe system model, using AlKα radiation of 250W X-ray tube as a radiation source with the energy of 1486.6 eV, 16mA ×12.5 kV under working pressure lower than 1 ×10⁻⁸ Nm⁻². The fitting of the XPS curves was analyzed with multi-pack 6.0A software. UV-visible absorption spectra of the samples were obtained by using Shimadzu 3600, UV - visible NIR spectrophotometer using BaSO₄ as reference scatter. Photoluminescent spectral analysis was done using the Horiba Jobin Fluoro Max-4 instrument with a PMT voltage of 150V and slit set both at 2.5 nm.

1.3. Photocatalytic Activity of Catalyst. For the establishment of adsorption-desorption equilibrium on the catalyst surface, a dye solution with catalyst was stirred in dark for 20min. The reaction mixture was exposed to a visible light source of 400W high-pressure mercury vapor lamp (Osram, India) by placing it 20 cm away from the light source. Aliquots of samples were withdrawn at a certain regular time interval, through a 0.45 μm Millipore syringe filter. The filtrate was analyzed on a spectrophotometer at a wavelength of 517nm for percentage degradation studies of eosin yellow. To have a comprehensive idea of the reaction environment it is necessary to maintain the same for all the activity tests. Percentage degradation of the dye was calculated from the following equation:

Where *A*₀ is the initial absorbance of dye solution before degradation and *A* is the absorbance of dye solution at time *t*.

II. RESULTS AND DISCUSSIONS

2.1 XRD patterns of Ba²⁺ and Zr⁴⁺ Co-doped TiO₂ nanomaterial samples and undoped titania were prepared by the sol-gel method and calcined at 450°C shows in Fig.1. All the samples are in the anatase phase (JCPDS No.: 21-1272) with corresponding (1 0 1) plane at 2θ = 25.3° followed by 2θ of 37.7°, 47.9°, 54.1°, 55° and represents the planes (004), (200), (105), (211) anatase TiO₂ respectively. Moreover, it was observed that, when the dopant Ba²⁺ concentration increases from 0.25 to 0.5, it was not observed any respective peaks of barium oxide. After increasing the concentration of Ba²⁺ as 0.75 and 1.0, it was observed additional peaks at 23.84°, 34.1°, 42.19°, 46.78° which corresponds to the formation of BaCO₃ [18]. On the other side, there is also no detectable dopant Zr⁴⁺ related peaks were observed. Hence, the Zr⁴⁺ may be occupied substitutional sites of the TiO₂ crystal

structure and it is more electropositive than TiO₂ which favors the formation of less dense anatase phase [18]

2.2. Ultraviolet-Visible Diffuse Reflectance Spectroscopic Studies The UV-visible DRS spectrum of prepared samples was shown in Fig. 2. From the UV-visible DRS studies, the characteristic band for the prepared samples was in the range of 388 to 500 nm, and the bandgap energy (eV) for the selected samples calculated using $E=1240/\lambda$ (whereas λ is wavelength). The bandgap of synthesized undoped TiO₂ was found to be 3.17 eV which is comparable with the literature value. The co-doped samples showed bandgap ranging from 2.63 to 3.02 eV. Hence narrowing the bandgap, imparts the absorbance shifted from ultraviolet to the visible region. Thus, Redshift indicates more photogenerated e⁻/h⁺ pairs that could be excited by photons with less energy, lead to better photocatalytic efficiency in the visible region. Thus, the results confirmed that all the synthesized co-doped samples had reduced bandgap and are active in the visible region.

Catalyst	The crystallite size (nm)	Bandgap (eV)
0.75wt% Ba & 0.25wt% Zr-TiO ₂	20.15	2.689
Undoped	36.55	3.17

2.3 TEM image of 0.75 wt. % Ba and 0.25 wt. % Zr co-doped TiO₂ was represented in Fig. 3 and the average particle size was found to be 20.63nm. It is in good agreement with the results of crystallite size calculated by using the Scherer equation and the full width at half maximum of the (101) peak in the XRD patterns of the nanomaterial. Co-doping of Ba²⁺ & Zr⁴⁺ in TiO₂ brings in the decrease of the crystallite size of TiO₂ which leads to an increase of the surface area of the catalyst, which is a favorable precondition for higher photocatalytic activity.

Based on XRD data and trail photocatalytic activity studies, further characterization has been made for Ba & Zr co-doped nanomaterial which showed best in trail photocatalytic activity studies.

2.4. X-Ray Photoelectron Spectroscopic (XPS) Analysis.

XPS Analysis of Ba & Zr co-doped nanomaterial was carried out to confirm the presence of Ba and Zr and investigate their chemical state. High-resolution XPS spectra of Ba & Zr co-doped nanomaterial with elemental analysis of Ti, O, Ba, and Zr were represented in Figure 4. The co-doped

showed two peaks of Zr_{3d5/2} and Zr_{3d3/2} are absorbed with a binding energy of 178.332 and 181.063 eV respectively, this can be attributed to Zr⁴⁺. From the above XPS results, a 3d peaks at 781.171eV and 795.874eV corresponding to 3d5/2 and 3d3/2 respectively are assigned as Ba²⁺ and does not absorb into the TiO₂ being it is high atomic radii than Ti. The XPS spectra of undoped TiO₂ show spin-orbit doublet peaks of Ti 2p3/2 and 2p1/2 located at 459.0 and 464.7 eV which indicating the presence of Ti⁴⁺ in the synthesized nanopowders[19,20]. Thus, the presence of zirconium has a certain influence on Ti⁴⁺ pulling the electrons in Ti–O–Ti bond, a bit away from the Ti atom, thus causing a little rise in Ti 2p3/2 binding energy. Thus, XPS data has confirmed that there is substitutional doping of Zr in the TiO₂ network.

2.5. Photoluminescent Spectral Studies

The fundamental reactive species during the photocatalytic reaction is Hydroxyl radical which is responsible for the oxidative decomposition of pollutants. To investigate the production of ·OH one of the methods is the photoluminescence technique. Coumarone is used as a fluorescent probe, which on reaction with ·OH results in the formation of 7-hydroxy coumarone [21]. In this technique, 0.1 gm of catalyst is dispersed in 10ppm of coumarone 100ml aqueous solution in acidic conditions and exposed to visible light radiation. For every 30 min, the reaction solution was filtered and photoluminescent intensity was measured from 350 to 600 nm. The photoluminescent spectra of the generated 7-hydroxy coumarin with maximum absorption at 450 nm showed in Fig.5. An increase of photoluminescent intensity was observed linearly with increasing irradiation time. However, no maximum absorption is observed for the sample in absence of irradiation (0 min). Hence the produced ·OH at the catalyst surface was proportional to the irradiation time. The results further confirmed that the synthesized sample Ba & Zr co-doped TiO₂ showed a better rate of formation of ·OH.

2.6. Photocatalytic Degradation of Eosin Yellow

Photocatalytic degradation of eosin yellow was performed using the procedure given in section 1.3. A blank test without photocatalyst is also performed and there was no change of dye concentration observed. The photocatalytic performance depends on certain parameters, these parameters are dopant concentration, catalyst dosage, pH of the solution, and initial dye concentration hence optimization of these parameters must be necessary to be cost-effective.

2.6.1. Effect of Dopant Concentration

Photocatalytic degradation studies of different synthesized various dopant concentrations of catalysts on eosin yellow are presented in Fig.6(a). All the co-doped samples showed higher photocatalytic activity than undoped titania, under visible light irradiation. So, it is evident that co-doping enhances the photocatalytic performance of TiO₂. Among all the co-doped nanomaterials 0.75wt%Ba & 0.25wt% Zr co-doped TiO₂ showed a better percentage of photocatalytic degradation.

Regarding the above analysis, the optimal Ba and Zr content are so small hence with overdosage of dopant content in TiO₂, the number of e⁻/h⁺ recombination centers will increase which is accompanied by low photocatalytic activity.

2.6.2. Effect of pH. Figure 6(b) represents the percentage of degradation of eosin yellow as a function of time at different pH values. A nanomaterial exhibiting the best photocatalytic performance of 0.75wt% Ba & 0.25wt% Zr co-doped TiO₂ was selected and experiments were conducted for finding the optimum pH at a constant dye concentration of 10ppm and catalyst dose of 0.1gm. As we have observed from the figure that photodegradation of this anionic dye was faster at pH 2. During photocatalytic degradation, electrostatic interactions among a semiconductor surface, substrate, and charged radicals strongly depend on the pH of the solution. At a lower pH environment, the positive charge on the TiO₂ surface increases which enhances the adsorption of dye molecules on the surface of the catalyst, in addition to minimize the e⁻/h⁺ recombination. But at higher pH TiO₂ surface develops negative charges that occur repulsion with a dye molecule that imparts in low adsorption of molecule leading to low degradation efficiency.

2.6.3. Effect of Catalyst Dosage

An optimum catalyst concentration must be decided to avoid wastage of catalysts and ensure the total absorption of photons. Photocatalytic degradation was carried out upon using varying dosage from 0.25-0.3gm of the selected co-doped TiO₂ nanomaterial at pH 2 is represented in fig.6. Linear increase rate of degradation was observed with an increase in the amount of catalyst up to 0.2gm.

The number of photons absorbed by the catalyst is high as the catalyst dosage is increased, which in turn increases the generation of electrons and holes and thus increases the number of hydroxyl radicals. Hence it absorbs also more dye molecules. However, beyond 0.2gm of catalyst dosage, photocatalytic activity decreased due to the turbidity

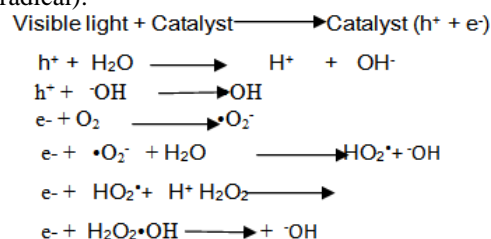
acts as a blanket that is a restriction of light penetration. Since high catalyst dosage significantly affects the dispersion.

2.6.4. Effect of Initial Concentration of Dye.

To decide the optimum initial dye concentration at a fixed catalyst dosage and pH, experiments were conducted with different dye concentrations of 5, 10, 15, and 20ppm, and results are represented in Fig.6(d).

The optimum initial concentration of dye was found to be 10ppm and a further increase in dye concentration decreased the rate of degradation. For this reason, as the dye concentration increases, the corresponding ratio of reactive species ($\cdot\text{OH}$) may not be formed at the fixed catalyst dosage. Restriction of surface-active sites for the catalytic reaction may also control the degradation of eosin yellow.

2.7. The mechanism in the Release of $\cdot\text{OH}$ (hydroxyl radical).



III. CONCLUSION

Barium and zirconium were effectively co-doped TiO₂ and its photocatalytic activity was studied for the degradation of eosin yellow under visible light. All the synthesized samples were in the anatase phase and the band-gap has been reduced. Co-doping improved the trapping of electrons inhibiting e⁻/h⁺ recombination during the photocatalytic process. Among all the synthesized catalysts 0.75wt.% Ba and 0.25wt.% Zr co-doped TiO₂ exhibited excellent photocatalytic activity under visible light due to a large shift in the bandgap, high crystalline anatase phase, and effective separation of electrons and holes. 100% degradation of eosin yellow with an initial concentration of 10ppm was achieved in 20 min at pH 2 with a catalyst dosage of 0.1gm. The experimental results revealed that eosin yellow can be effectively degraded by Ba & Zr co-doped TiO₂.

REFERENCES

- [1]. R Ahmed and Kumar R., Adsorptive removal of Congo red dye from aqueous solution using bael shell carbon, Appl. Surf. Sci. Vol. 257, (2010), 1628-1633.

- [2]. N.S. Arul, D. Mangalaraj, J.I. Han, Photoelectrochemical degradation of eosin yellowish dye on exfoliated graphite–ZnO nanocomposite electrode. *J. Mater. Sci. Mater. Electron.* 26, (2015), 1441–1448.
- [3]. B.R. Babu, A.K. Parande, S. Raghu, T. PremKumar, Cotton Textile Processing: Waste Generation, and Effluent Treatment. *J. Cotton Sci.* 11, (2007), 141–153.
- [4]. E. Erdem, G. C. Olgecen, R. Donat. Adsorption of phenol from aqueous solutions by *Luffa cylindrica* fibers, Kinetics, isotherm, and thermodynamic studies. *J. Colloid Interface Sci.* 282, (2005), 314–319.
- [5]. H. Hameed, J. Hazard. Spent tea leaves: a new non-conventional and low-cost adsorbent for removal of basic dye from aqueous solutions. *Mater.* 161, (2009), 753–759
- [6]. N. Emmanuel, G. Kumar, *Environ. Chem.* Photo detoxification of solubilized vat dye effluent using different pH ranges. *Lett.* 7, (2009), 375–379.
- [7]. J. Rathousky, V. Kalousek, M. Kola's, J. Jirkovsky, Mesoporous films of TiO₂ as efficient photocatalysts for the purification of water. *Photochem. Photobiol. Sci.* 10, (2011), 419–424.
- [8]. L.M. AL-Harbi, E.H. El-Mossalamy, Mod. Effect of RE Dopant (Ce & Tb) on PL and Crystallite size of Lanthanum Phosphor (LaPO₄). *Appl. Sci.* 5, (2011), 130–135.
- [9]. N. Banerjee, The design, fabrication, and photocatalytic utility of nanostructured semiconductors: focus on TiO₂-based nanostructures. *Nanotechnol. Sci. Appl.* 4, (2011), 35–65
- [10]. Guido Rothenberger, Jacques Moser, Michael Graetzel, Nick Serpone, Devendra K. Sharma. Charge carrier trapping and recombination dynamics in small semiconductor particles, *Journal of the American Chemical Society* 107 (26), (1985), 8054–8059
- [11]. Narayanan N. Binitha, Zahira Yaakob, Ramakrishnan Resmi Influence of synthesis methods on zirconium doped titania photocatalysts *Cent. Eur. Journal of Chem.* 8(1) 2010, 182–187
- [12]. EW, McFarland; H, Metiu; Eric W. M. Farland and Horia Metiu. *Catalysis by doped oxides.* *Chem Rev*, 113: 2013, 4391–4427.
- [13]. A. Fujishima; X. Zhang; D.A, Tryk; TiO₂ photocatalysis and related surface phenomena. *Surf Sci. Rep.* 63: 2008, 515–582.
- [14]. R. Asahi; T. Morikawa; T. Ohwaki; K. Aoki; Y. Taga; Visible-light photocatalysis in nitrogen-doped titanium oxides. *Science*, 293, 2001, 269–271.
- [15]. R. Khan; S. Kim; W. Kim; T.J. Lee; H. S, Preparation and application of visible-light-responsive Ni-doped and SnO₂-coupled TiO₂ nanocomposite photocatalysts. *Bull; Korean Chem. Soc.*, 28, (2007), 1951
- [16]. T. S. Anirudhan and S. R. Rejeena Photocatalytic Degradation of Eosin Yellow Using Poly(pyrrole-co-aniline)-Coated TiO₂/Nanocellulose Composite under Solar Light Irradiation *Hindawi Publishing Corporation Journal of Materials Volume 2015, Article ID 636409, 11*
- [17]. Jongee Park, Derya Kapsuz, Abdullah Ozturk) Sol-gel synthesis and photocatalytic activity of B and Zr co-doped TiO₂. *J. of Physics and Chemistry of Solids* 74, (2013), 1026–1031
- [18]. N. Venkatachalam, M. Palanichamy, V. Murugesan, Sol-gel preparation and characterization of alkaline Earth metal doped nano TiO₂ efficient photocatalytic degradation of 4-chlorophenol, *Journal of molecular catalysis A: chemical* 273, (2007) 177–185
- [19]. M. Zhang, X. Yu, D. Lu, and J. Yang, Facile synthesis and enhanced visible light photocatalytic activity of N and Zr co-doped TiO₂ nanostructures from nanotubular titanate precursor, *Nanoscale Research Letters* 8, (2013), 1–8.
- [20]. H. Czili and A. Horv'ath, "Applicability of coumarin for detecting and measuring hydroxyl radicals generated by photoexcitation of TiO₂ nanoparticles. *Applied Catalysis B: Environmental*, vol. 81, no. 3–4, (2008), 295–302,

Table 1. Shows crystallite size, Band gap and BET surface area of the prepared co-doped catalysts.

Fig.1. XRD pattern of the synthesized undoped and 0.75 wt% of Ba²⁺ & 0.25 wt% Zr⁴⁺ co-doped TiO₂

Fig.2. The DRS spectra of undoped TiO₂, and 0.75 wt% of Ba²⁺ & 0.25 wt% Zr⁴⁺ co-doped TiO₂.

Fig. 3. TEM images of (a) undoped TiO₂ (b) 0.75 wt% of Ba²⁺ & 0.25 wt% Zr⁴⁺ co-doped TiO₂.

Fig. 4. (a) XPS survey spectrum of co-doped TiO₂ (b) high resolution spectrum of C1s (c) O1s (d) Ti2p (e) Ba 3d and (f), Zr3d respectively.

Fig. 6. Effect of dopant concentration on photocatalytic activity of co-doped titania on the % degradation of eosin yellow. Here, catalyst dosage 0.1 gm, pH=10, & [eosin yellow] = 10 ppm.

Fig.7. The effect of pH on the %degradation of eosin yellow by Ba²⁺&Zr⁴⁺ co-doped TiO₂. Here, catalyst dosage =0.1gm and [eosin yellow] = 10ppm.

Fig. 8. Effect of catalyst dosage on the %degradation of eosin yellow by 0.75 wt% Ba²⁺& 0.25 wt% Zr⁴⁺ co-doped TiO₂. Here, pH=10 and eosin yellow =10 ppm.

Fig.9.The effect of the initial concentration of dye on the % degradation of eosin yellow. Here,pH = 2, catalyst dosage =0.1gm.

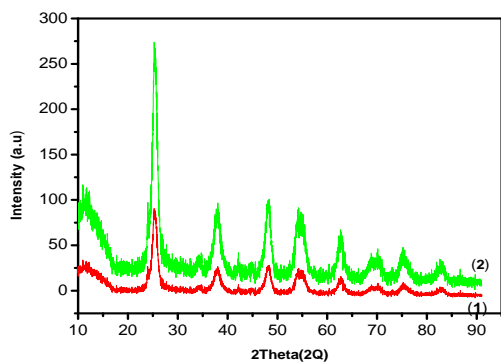


Fig.1. XRD pattern of the synthesized (1)undoped and (2) 0.75wt% of Ba²⁺ & 0.25 wt% Zr⁴⁺ co-doped TiO₂

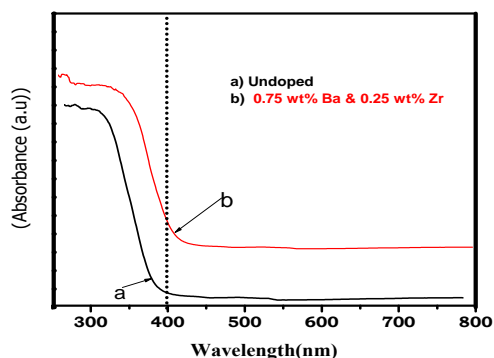


Fig.2.The DRS spectra of undoped TiO₂, and 0.75wt% of Ba²⁺ & 0.25 wt% Zr⁴⁺ co-dopedTiO₂.

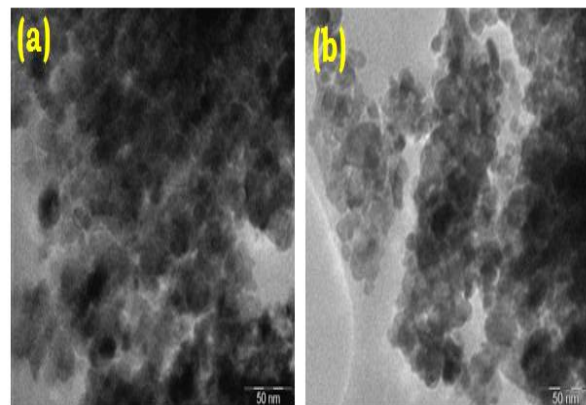


Fig. 3.TEM images of (a) undoped and (b)0.75wt% of Ba²⁺ & 0.25 wt% Zr⁴⁺ co-doped TiO₂.

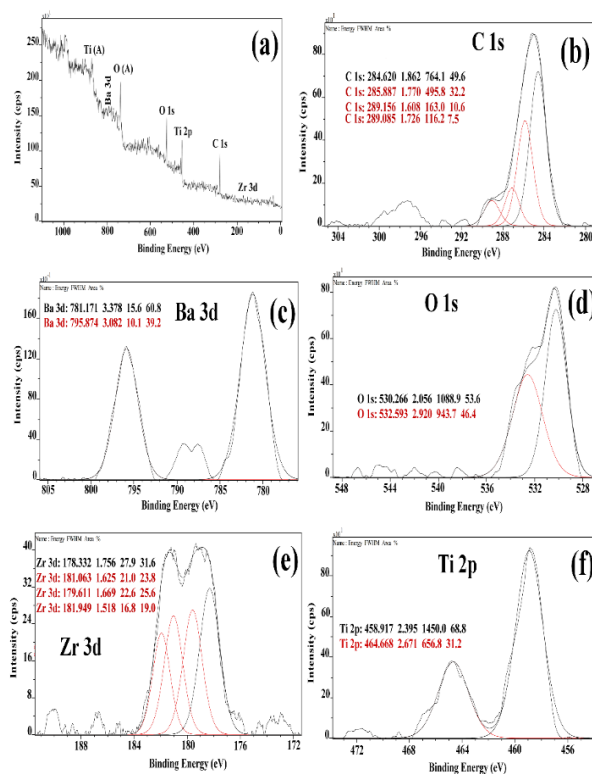


Fig. 4. (a) XPS survey spectrum of co-doped TiO₂ (b) high resolution spectrum of C1s (c)Ba3d (d) O1s (e) Zr 3d and (f) Ti2p, respectively.

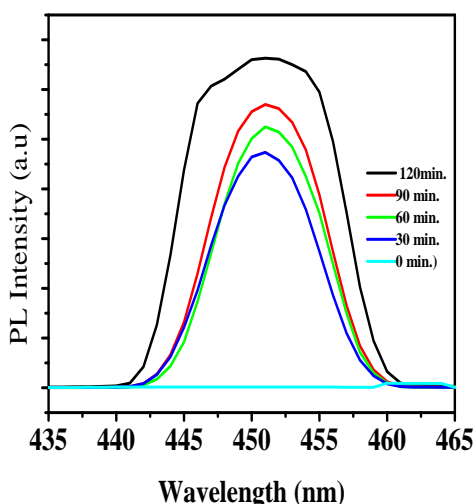
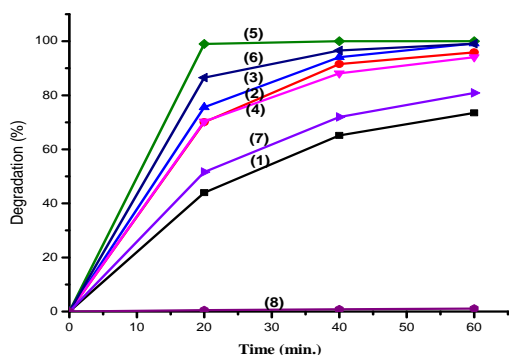


Fig.5. Photoluminescence spectra of Ba and Zr co-doped catalyst



1. 1wt% Ba & 0.25wt% Zr -TiO₂
2. 0.25wt% Ba & 1wt% Zr -TiO₂
3. 0.5wt% Ba & 0.5wt% Zr -TiO₂
4. 0.25wt% Ba & 0.75 Zr wt% Zr- TiO₂
5. 0.75wt% Ba & 0.25 wt% Zr - TiO₂
6. 0.5wt% Ba & 1wt% Zr - TiO₂
7. 1wt% Ba & 0.5wt% Zr - TiO₂
8. Undoped (TiO₂)

Fig. 6. Effect of dopant concentration on photocatalytic activity of co-doped titania on the % degradation of eosin yellow. Here, catalyst dosage =0.1gm, pH=10, & eosin yellow=10ppm

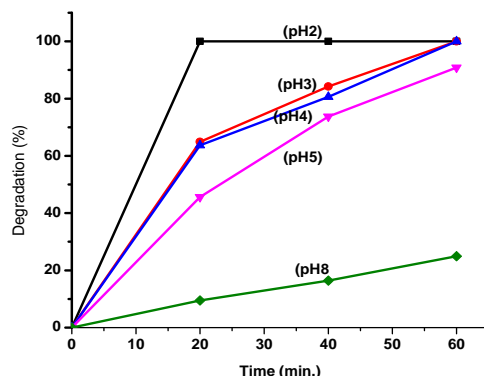


Fig.7. The effect of pH on the % degradation of eosin yellow by Ba²⁺ & Zr⁴⁺ co-doped TiO₂. Here, catalyst dosage =0.1gm and eosin yellow = 10ppm.

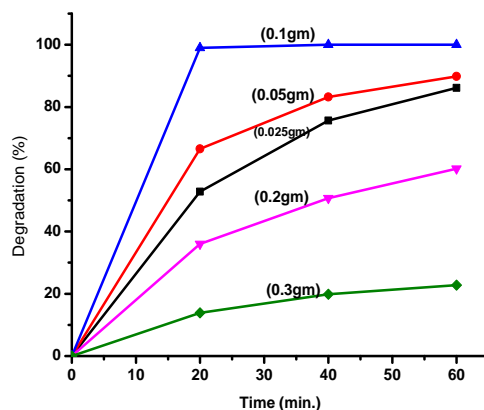


Fig. 8. Effect of catalyst dosage on the % degradation of eosin yellow by 0.75 wt% Ba²⁺ & 0.25 wt% Zr⁴⁺ co-doped TiO₂. Here, pH=10 and eosin yellow =10 ppm.

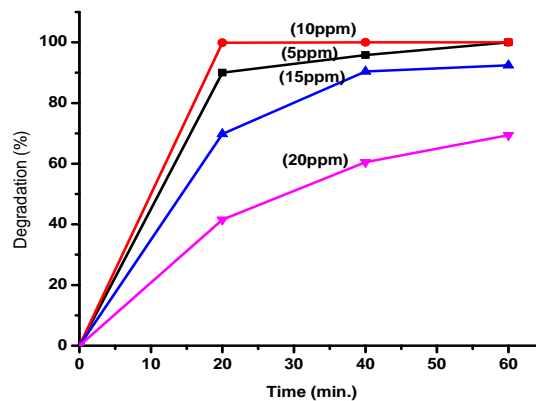


Fig.9. The effect of the initial concentration of dye on the % degradation of eosin yellow. Here, pH = 2, catalyst dosage =0.1gm.